Journal of Applied Science and Engineering, Vol. 21, No. 3, pp. 317–330 (2018) *DOI: 10.6180/jase.201809_21(3).0003*

Removal of Malachite Green from Aqueous Phase Using Coconut Shell Activated Carbon: Adsorption, Desorption, and Reusability Studies

S. A. Haji Azaman, A. Afandi, B. H. Hameed and A. T. Mohd Din*

School of Chemical Engineering, Engineering Campus, Universiti Sains Malaysia, 14300 Nibong Tebal, Pulau Pinang, Malaysia

Abstract

The use of coconut shell activated carbon (CSAC) as a potential adsorbent for malachite green (MG) dye from aqueous solution was investigated in this study. The effect of various factors, such as initial dye concentration, contact time, pH, and solution temperature were studied. The interaction between dye molecule and CSAC absorbent was strongly influenced by the pH of the solution. Maximum adsorption of MG was obtained at pH 6.5, while, the point of zero charge (pH_{zpc}) of CSAC was obtained at pH 6.1. The Langmuir, Freundlich, and Temkin isotherms were used to describe the adsorption equilibrium of the MG. The maximum monolayer adsorption capacities, Q_m, were increased with increment in temperature. The kinetics of adsorption followed a pseudo-second-order kinetic model. The intraparticle diffusion model was evaluated to determine the mechanism of the adsorption process. Based on the Boyd plots, the adsorption of MG on the CSAC absorbent was mainly governed by film diffusion. Thermodynamic parameters, such as $\Delta G°$, $\Delta H°$, and ΔS were determined and it was found that MG adsorption on CSAC was spontaneous and endothermic in nature. The conducted reusability test disclosed the decreasing CSAC performance from 98% MG removal down to 89% MG removal after 5 consecutive adsorption/desorption cycles.

***Key Words*:** Intraparticle Diffusion, Film Diffusion, Boyd, Temkin

1. Introduction

Synthetic dyes have been widely used in textiles, leather, paper, wool, cosmetics, and printing industries, and they contain large amount of solids [1]. It was reported that 7×10^5 tonnes of synthetic dyes are produced annually around the world. Approximately 20% of the dyes used during manufacturing and processing operations are finally discharged into industrial wastewater. Two-thirds of the dye consumption are dominated by the textile industries, which dispose high amount of dyes, of up to 146,000 tonnes per year [2]. The presence of dye pollutants in natural water bodies can have severe and hazardous impacts on aquatic life because of the mutagenic, carcinogenic, allergenic, and toxic nature of dyes [3]. The existence of metal ions, aromatic rings, and chlorides in dye structures had enhanced their toxicity, carcinogenicity, as well as their teratogenic and mutagenic properties [1]. Among other dyes, malachite green (MG) is the most extensively used raw material as a colorant in various industrial applications. MG is used as a medical disinfectant, food additive, and food colouring agent, and it is also used in silk, wool, jute, leather, cotton, acrylic, and paper industries [4–6]. Apart from its numerous applications, the hazardous and carcinogenic effects of MG have also been reported by several studies [7]. It is extremely hazardous to mammalian cells and it has been identified as a liver tumour promoter. In humans, it can lead to toxicity to the respiratory system if inhaled and may cause infertility. It also reduces light penetration

*Corresponding author. E-mail: chazam@usm.my

into water and impedes photosynthetic activity in aquatic plants [7]. Hence, it is important to remove MG due to its hazardous effects on ecological systems and public health.

The removal of MG dye with a complex chemical structure from wastewater is a difficult task. The main reason is because MG has a high resistance to oxidizing agents and light, and has low efficiency on biological precipitation and chemical precipitation [8]. Several methods can be used to remove dye, which include coagulation and flocculation [9], adsorption [10], biosorption [11], electrochemical techniques [12], and fungal decolonization [13]. Other traditional methods, such as reverse osmosis, electrodialysis, ultrafiltration, and ion-exchange, have several disadvantages, which include incomplete removal, high energy generation of sludge, as well as high capital and operating costs [10]. Among these methods, adsorption is the most effective method for the removal of dyes because it is low cost, has a simple design, easy to handle, insensitive to toxic substances, and can completely remove dye pollutants [14].

In recent years, various low-cost absorbents from agricultural wastes/by-products have been used for dye removal. These absorbents are very economical, eco-friendly, are renewable, cheaper, with excellent dye removal ability, and are abundantly available. For these reasons, many researchers have tried to prepare activated carbons from agricultural wastes, such as banana peels, plum kernels, oil palm shells, tealeaves, and rice husks [15]. Coconut is largely planted along the coastal line of Peninsular Malaysia. Hence, high amount of solid wastes in the form of fibres and shells are produced annually. Utilisation of these wastes as an activated carbon precursor is highly recommended to moderate the solid waste disposal issue, as well as to generate local economy. This study reports the capabilities of CSAC as a low-cost absorbent for MG removal from aqueous solution. A series of experiments, namely, the effect of initial MG concentration, pH, absorbent dosage, and temperature on MG adsorption were studied. The kinetics, adsorption isotherms, and thermodynamic studies were also conducted and reported. Furthermore, cyclical desorption and regeneration of CSAC were performed to demonstrate the reusability of the adsorbent.

2. Materials and Methods

2.1 Materials

The adsorbate (malachite green) with chemical formula of $C_{23}H_{25}N_2$ (MW = 364.92 g/mol) was supplied by Sigma Aldrich, Malaysia. A stock solution of 100 mg/L was prepared by dissolving 0.1 g of MG into 1 Lof distilled water. The desired concentrations were prepared by diluting the MG stock solution with distilled water. The coconut shell activated carbon (CSAC), in a granular form with size ranging between 2.38–0.595 mm, was obtained from a local supplier, Ki Carbon Solutions. Hydrochloric acid, HCl (Fuming, 37 wt%) and sodium hydroxide, NaOH (pellets) were purchased from R & M Chemicals (Malaysia).

2.2 CSAC Characterisation

The physicochemical properties of CSAC, such as surface area, micropore area, and total pore volume, were obtained using a surface area analyser (Micrometrics ASAP 2010, USA) at 77 K. The FTIR spectra of CSAC, before and after MG adsorption, were compared and analysed in the range of 400–4000 cm^{-1} to determine the surface functional groups. The FTIR analysis was conducted using an FTIR spectrophotometer (Shimadzu IR Prestige-21, Japan). Proximate analysis was conducted using a thermogravimetric analyser (TGA) (Model Perkin Elmer TGA7, USA) to determine the amount of moisture, volatile organic, as well as the fixed carbon and ash contents. Scanning electron microscope (SEM), with EDX analysis (SEM Quanta FEG 450, USA), were used to study the surface morphology of the samples.

2.3 Adsorption Studies

To obtain the adsorption equilibrium profiles of MG on CSAC, a series of liquid phase, batch adsorption experiments were performed. The effects of the following parameters; initial concentration, contact time, pH of the solution, adsorbent dosage, and temperature were investigated in this work. The concentration of MG solution, before and after the adsorption experiments, was inspected using a UV-Vis spectrophotometer (Shimadzu UV1800, Japan) at λ_{max} = 618 nm. The adsorbed amounts of MG at time, q_t (mg/g) and at equilibrium condition, q_e (mg/g) were calculated according to the following Eq. 1 and Eq. 2, respectively:

$$q_t = \frac{(C_0 - C_t)V}{W} \quad (1)$$

$$q_e = \frac{(C_0 - C_e)V}{W} \quad (2)$$

where C_0 and C_e are the concentrations (mg/L) of MG dye at initial and equilibrium conditions, respectively. V is the volume (L) of the solution, and W is the weight (g) of the adsorbent used.

2.3.1 Effect of Solution pH

The effect of pH of the MG dye solution was evaluated by varying the initial pH of the solution, ranging between 2.5 to 6.5. The pH was adjusted by using 0.1 M HCL and 0.1 M NaOH solutions. A bench-top digital pH meter was used to measure the changing pH value. The initial MG dye concentration, temperature, and adsorbent dosage were kept constant at 50 mg/L, 303 K, 0.1 g, respectively. The removal percentage of MG was calculated using the following Eq. 3:

$$Removal\ (\%) = (C_0 - C_e) / C_0 \times 100 \quad (3)$$

2.3.2 Effect of Initial MG Dye Concentration, Contact Time, and Solution Temperature

For each set, 100 mL of MG dye solution of known concentration (10–50 mg/L) were poured into 250 mL flasks. CSAC, weighing at 0.1 g, was added into each flask. These flasks were placed in a water bath shaker at 303 K and shaking speed of 50 rpm. This procedure was repeated to study the effect of solution temperature by increasing the temperature to 313 K and 323 K, respectively.

2.3.3 Effect of Adsorbent Dosage

The effect of adsorbent dosage was studied by varying the amount of adsorbent. CSAC (0.1–0.5 g) was added into 250 mL flasks containing 100 mL of the 50 mg/L MG dye solution and the pH was adjusted using 0.1 M HCl and 0.1 M NaOH. Then, the solution was shaken at 50 rpm at a constant temperature of 303 K until equilibrium has been reached.

2.4 Determining pH_{zpc}

The point of zero charge (pH_{zpc}) of CSAC was studied using the pH titration procedure. The initial pH of 50 mL of 0.01 M NaCl solution was adjusted to initial pH values that ranged between 2 and 11 by using 0.1 M HCl and 0.1 M NaOH solutions. Next, 0.15 g of CSAC was added into each solution with the adjusted pH value and was left for 48 hours. The final pH was measured and the data were plotted, accordingly.

2.5 Desorption and Reusability Studies

Solvent desorption method was conducted to regenerate the used adsorbents for further dye removal. The desorption and regeneration experiments were performed in batch mode. Ethanol/water mixture was used as the desorption solution. First, used CSAC was obtained by conducting an adsorption experiment in 100 mL of MG dye solution (500 mg/L) at 323 K for 24 hours (pH 6.5, 0.1 g of CSAC). Next, the used CSAC was immersed in the ethanol/water mixture, with different concentrations ranging from 50% (50:50 v/v) to 90% (90:10 v/v) at 303 K, 308 K, 313 K, 318 K, and 323 K. The reusability of the CSAC was investigated by conducting five consecutive adsorption-desorption cycles. The percentage of MG desorption was evaluated using the following Eq. 4:

$$R(\%) = \frac{m_{des}}{m_{ads}} \times 100 \quad (4)$$

where m_{des} (mg/g) and m_{ads} (mg/g) are the amounts of desorbed and adsorbed MG, respectively [16].

2.6 Non-linear Error Functions

The validity of the adsorption isotherm models was evaluated using the coefficient of determination (r^2) and the sum-of-square-error (SSE), as shown by the following Eq. 5 and Eq. 6, respectively:

$$r^2 = \frac{\sum (q_{e,cal} - q_{e,ave})^2}{\sum (q_{e,cal} - q_{e,ave})^2 + \sum (q_{e,cal} - q_{e,\exp})^2} \quad (5)$$

$$SSE = \sqrt{\left(\left(\sum (q_{e,\exp)} - q_{e,cal} \right) \right)^2 / N} \quad (6)$$

where $q_{e,cal}$ is the amount of adsorbate adsorbed at equilibrium, as calculated from the model (mg/g), $q_{e,exp}$ is the equilibrium value obtained from the experiment (mg/g), and N is the number of data points. The non-linear error functions were solved using the SOLVER add-on

function in Microsoft Excel spreadsheet.

3. Results and Discussion

3.1 Characterisation of CSAC Adsorbent

Based on the TGA results, it was found that moisture content, volatile matter, and the fixed carbon and ash contents were 18.49%, 3.75%, 73.47%, and 4.28%, respectively. High fixed carbon content, with low ash value, are favourable characteristics for the activated carbon [17]. Surface area properties of the CSAC adsorbent are shown in Table 1. The BET results revealed that the measured total surface area was comparable to the value reported elsewhere [18]. FTIR analysis was also used to determine the functional groups of the adsorbent. The FTIR spectra of the raw and used CSAC samples are presented in Figure 1. There was no significant difference between the before (CSAC-RAW) and after adsorption (CSAC-USED) of MG. The spectrum shows a band at around 3500 cm^{-1}, which indicates the presence of hydroxylfunctional groups on the surface of CSAC. The peaks at 1630 cm^{-1} and 1622 cm^{-1} can be attributed to carbonyl groups (C=O). The peaks at 1384 cm^{-1} and 1388 cm^{-1} were due to the presence of C=H aliphatic bending. SEM images of raw CSAC adsorbent are shown in Figure 2. The SEM images show the uneven surface and porous structure of the CSAC adsorbent. The heterogeneous pore openings can be attributed to CSAC's high surface area, which acted as transport pores and active sites for the adsorption of MG. A similar observation on textural properties of coconut shell-based activated carbon was reported in a previous work [19].

Table 1. Surface area properties of CSAC absorbent

Total surface area[a]	Micropore surface area[b]	Total pore volume[c]	Micropore volume[d]	Average pore diameter[e]
1118.74	835.83	0.53	0.40	18.76

[a] BET surface area (m^2/g), [b] t-plot micropore surface area (m^2/g), [c] Total pore volume (cm^3/g), [d] Micropore volume (cm^3/g), [e] BET average pore diameter 4 V/A (nm).

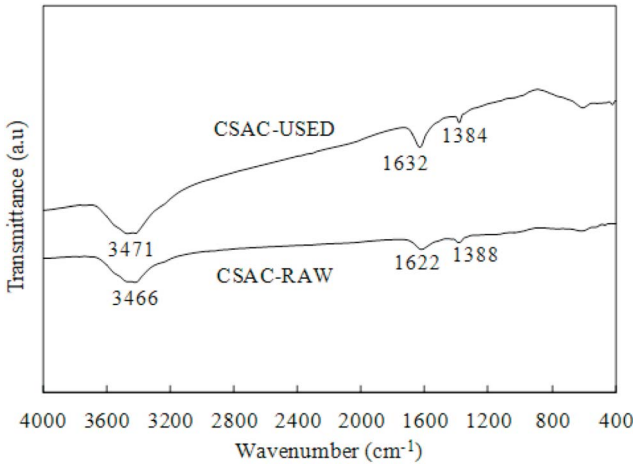

Figure 1. FTIR spectra of raw and used CSAC absorbent.

3.2 Effect of Solution pH

The pH of the solution can have a significant effect on the efficiency of the adsorption process. It controls the surface charge of the adsorbent, influences dye chemistry, dissociates functional groups of the adsorbent on the active sites, and capable of ionising the adsorbing molecules in the solution [2]. In this study, the MG solution became colourless at alkaline conditions. A similar observation was reported elsewhere [20]. Hence, the effect of pH on the removal of MG was only conducted in the acidic range up to pH 6.5. The effect of pH on the MG/CSAC adsorption system is illustrated in Figure 3.

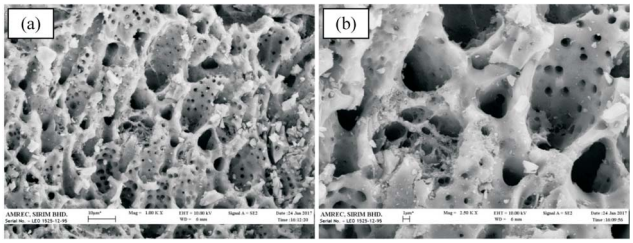

Figure 2. SEM images of CSAC absorbent at (a) ×1k magnification and (b) ×2.5 k magnification.

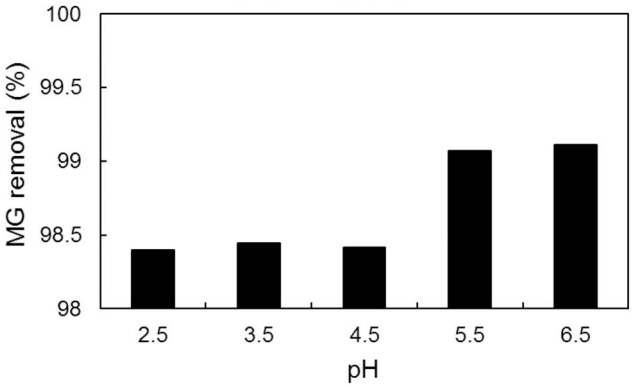

Figure 3. Effect of pH on removal of MG using CSAC (conditions: adsorbent dose = 0.1 g, shaking speed = 50 rpm, contact time = 24 hours, temperature = 303 K).

The percentage of MG removal had increased slightly with increasing pH. The highest MG removal of 99.11% was obtained at pH 6.5. A similar result was reported for MG adsorption on pumice stone [20]. Cationic MG is a positively charged ion in aqueous solution. The MG's ability to adsorb onto the surface of the adsorbent is mainly controlled by its surface charges, which is closely associated to the pH of the solution. At lower pH values (2.5–4.5), the number of H^+ ions would increase in the system. Subsequently, the adsorption of the positively charged ions in MG to the surface of the adsorbent would be reduced. At higher pH (4.5–6.5), the number of H^+ ions would decrease, which would lead to an increase in the number of negatively charged sites. Increasing the pH value has resulted in a higher percentage of MG removal due to the attraction between the positively charged ions in MG and the excess OH^- ions in the system, and the high number of OH^- ions on the surface of the adsorbent [10,21]. A strong electrostatic attraction had also occurred between the negatively charged adsorbent surface and the positively charged MG, which resulted in a maximum uptake of MG from wastewater [5]. The point of zero charge of the CSAC adsorbent was evaluated at pH 6.1. Hence, the CSAC's surface was positively charged when the pH of the solution was lower than 6.1, and it became negatively charged when pH was higher than pH 6.1. Thus, the solution pH must be kept at higher than the pH_{zpc} to gain favourable conditions for the adsorption of cationic dye [16]. Similar findings were reported on the adsorption of MG onto activated carbon prepared from the epicarp of *Ricinus communis* [5].

3.3 Effect of Initial Concentration and Contact Time

Figure 4 shows the plots of MG dye adsorption on the CSAC adsorbent as a function of contact time, with different initial concentrations at 303 K, 313 K, and 323 K. Initially, the adsorption rate was rapid for the first 60 minutes due to the adsorption of the cationic dye molecules onto the exterior surface of the adsorbent. Gradually, the adsorption rate began to decrease when the dye molecules began to experience mass transfer resistance while entering deep into the pores of the adsorbent [2,6]. At the beginning, the number of binding sites was higher and progressively, the sites became limited, which further reduced the adsorption rate. The adsorption process stopped when equilibrium was achieved, forming a plateau until the end of the adsorption time. Increasing amount of MG dye adsorbed onto CSAC was observed over time, until the solution had reached the equilibrium for all runs. A longer contact time to reach equilibrium was observed for MG solutions at higher concentrations.

The rate of adsorption is highly dependent on the initial concentration of the feed solution. Figure 4 shows that the amount of MG adsorbed had increased when the initial concentration of MG was increased. A comparable observation was reported on the adsorption of MG using iron nanoparticles loaded on ash [22]. This could

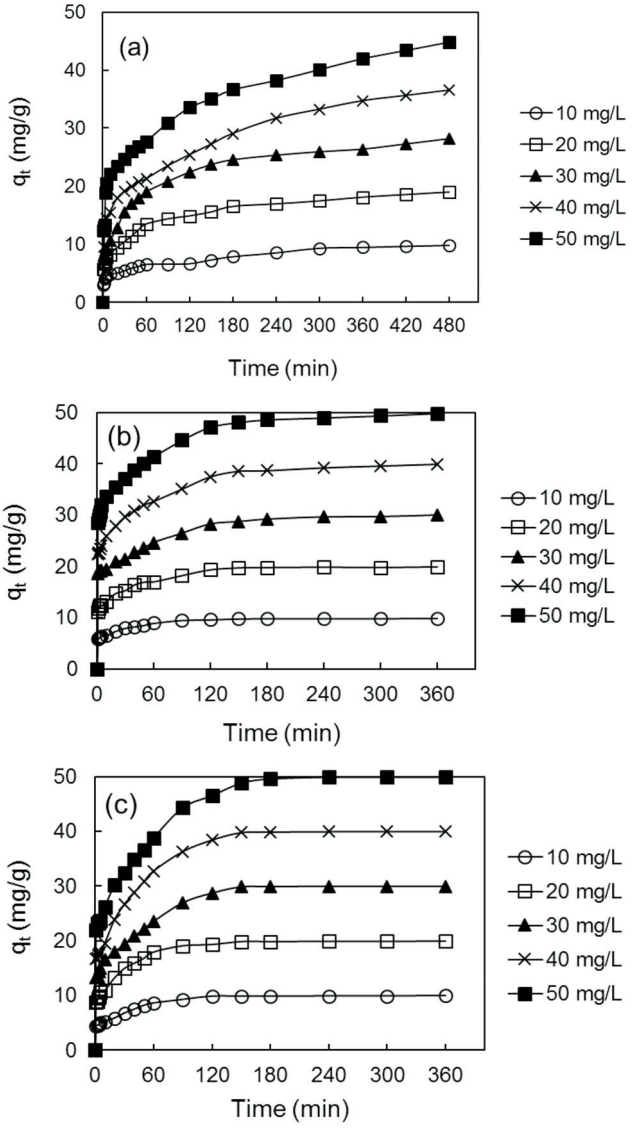

Figure 4. Adsorption profiles of MG on CSAC absorbent at (a) 303 K, (b) 313 K and (c) 323 K.

be explained by the increase in the driving force of the concentration gradient between the solid and aqueous phases [22].

3.4 Effect of Solution Temperature

Solution temperature is one of the factors that can strongly influence the equilibrium of dye uptake. Based on Figure 4, the MG uptake had increased with increasing solution temperature. A shorter time to equilibrium was observed when the temperature was increased from 303 K to 323 K. A short contact time (120 minutes) was needed for 10 mg/L of MG solution at 323 K to achieve equilibrium. In comparison, longer contact times (150 and 420 minutes) were needed when the temperature was decreased to 313 K and 303 K, respectively. These trends have demonstrated that higher temperature is favourable for the removal of MG. This could be attributed to an increase in the diffusion rate of the adsorbate molecules across the external boundary layer and within the internal pores of the adsorbent due to the decreasing viscosity of the solution when the solution temperature was increased [23].

3.5 Effect of Adsorbent Dosage

Figure 5 shows the plot of MG removal against varying adsorbent dosage. The MG removal percentage has shown a rapid increase with increasing CSAC dosage of up to 0.3 g. No significant changes in MG removal were observed when the adsorbent dosage was increased to 0.5 g. A similar trend was highlighted in the adsorption of MG from aqueous solutions using cyclodextrin-based adsorbent [24]. However, the amount of adsorbed MG on the CSAC had decreased with increasing adsorbent dosage (see Figure 6). It can be summarised that increasing the adsorbent dosage up to 0.3 g had increased the number of active binding sites, hence increasing dye uptake onto the surface of the adsorbent [25,26]. Further increase in the adsorbent dosage, however, had led to an excess of active sites. As the adsorption system progressed towards equilibrium, these active sites were left vacant and unoccupied due to insufficient number of adsorbates in the bulk phase. Hence, it was no longer operative to increase the amount of adsorbates adsorbed [25,27]. A shorter time to achieve equilibrium was also observed over increasing adsorbent dosage. Based on Figure 6, an equilibrium time of 420 min was reduced to 360 min and later, 300 min over increasing adsorbent dosage from 0.1 g to 0.3 g and 0.5 g, respectively.

3.6 Desorption and Reusability

The reusability of used adsorbents is very important for the economic feasibility of the adsorption process. In general, MG desorption efficiency of less than 20% was observed, as shown in Figure 7. The MG desorption efficiency had increased from 50% to 80% over increasing ethanol concentration. A slight decrease in MG desorption percentage was observed when ethanol concentration was increased to 90%. The maximum MG desorption was achieved at 80% (80:20, v/v) of ethanol/water mixture. Similar results were reported on the regeneration of porous magnetic microspheres using ethanol and

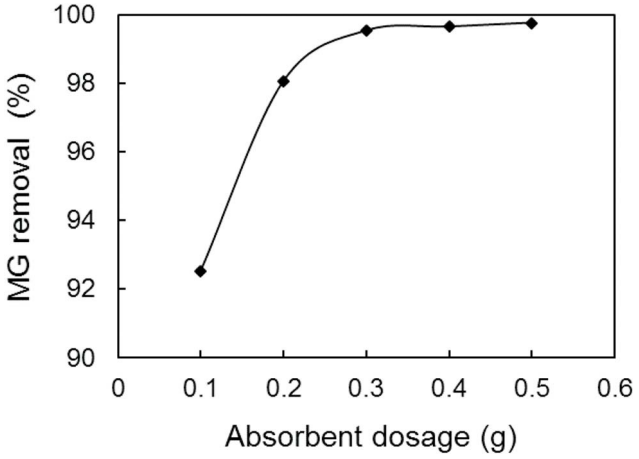

Figure 5. Removal percentage of MG at varying CSAC adsorbent dosage.

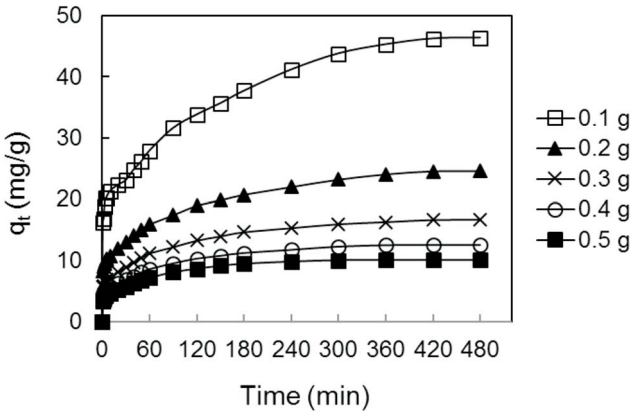

Figure 6. Amount of MG adsorbed on CSAC at varying adsorbent dosage.

water as co-solvent [28]. Temperature has been known to have a significant influence on the desorption process. Based on Figure 8, the desorption efficiency of MG had decreased with increasing temperature. A maximum desorption percentage of approximately 20% was observed at 303 K. The reusability of CSAC after five consecutive adsorption/desorption cycles is presented by Figure 9. The MG adsorption efficiency had slightly decreased from 98% to 89% at the end of the fifth cycle. The ability to withstand five consecutive adsorption/desorption cycles has proven that CSAC possesses a good adsorbent reusability characteristic, one of the important criteria in designing economical adsorption processes.

3.7 Two-parameter Adsorption Isotherm Fittings

Figure 10 shows the non-linear plots of the selected

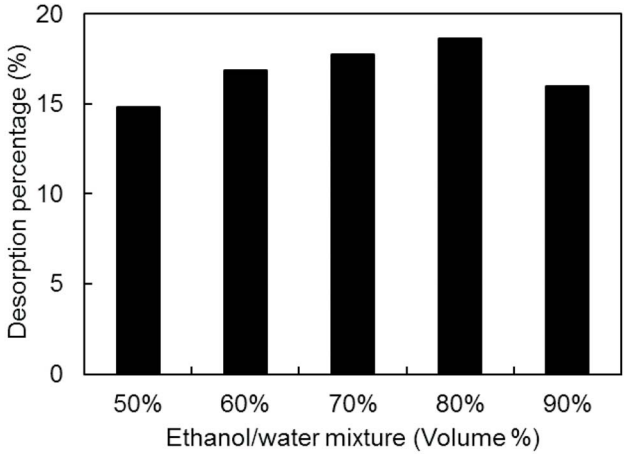

Figure 7. Desorption efficiency of MG from the used CSAC at different ethanol/water mixture concentrations.

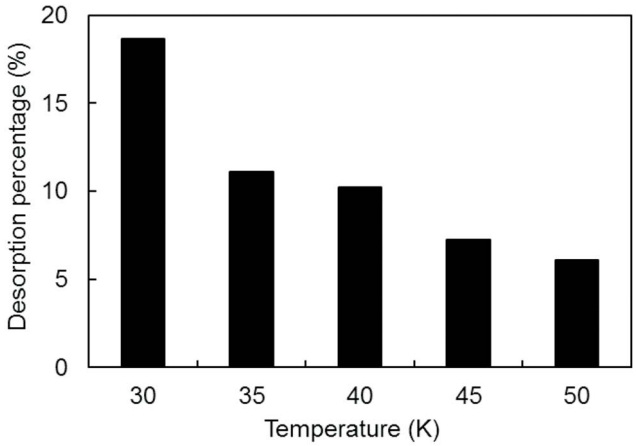

Figure 8. Desorption efficiency of MG from the used CSAC at different temperature.

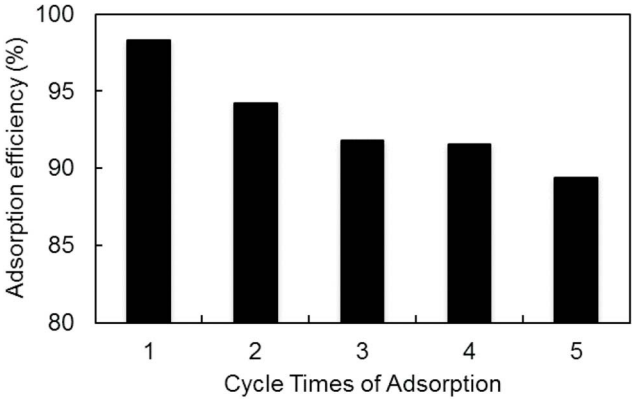

Figure 9. Adsorption/desorption cycle of used CSAC.

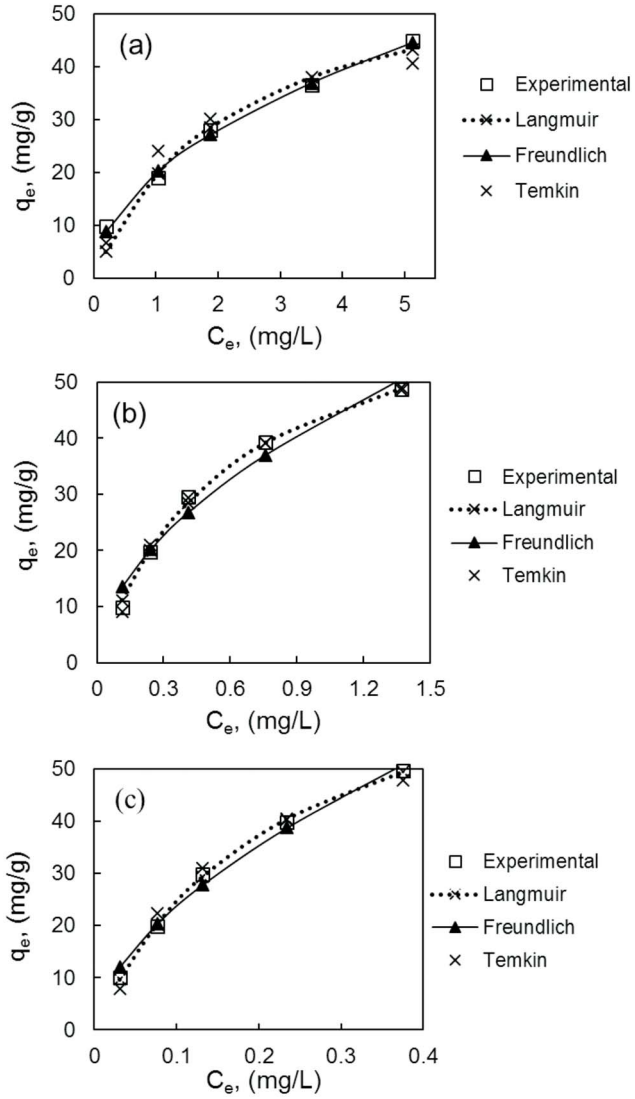

Figure 10. Non-linear plots of two-parameter adsorption isotherms at (a) 303 K, (b) 313 K, and (c) 323 K.

two-parameter adsorption isotherm models at 303 K, 313 K, and 323 K. The calculated isotherm constants and the resulting non-linear errors are presented in Table 2. R_L is the Langmuir separation factor, used to measure the preference of the adsorption nature. R_L and B_T are defined by the following Eq. 7 and Eq. 8, respectively [29]:

$$R_L = 1 / (1 + K_L C_o) \quad (7)$$

$$B_T = RT / b_T \quad (8)$$

where K_L and C_o are Langmuir constant (L/mg) and the highest initial dye concentration (mg/L), respectively. The value of constant B_T indicates the heat of adsorption. R and T are the universal gas constant (8.314 J (K mol)$^{-1}$) and temperature (K), respectively. The preference of the adsorption process can be interpreted as unfavourable ($R_L > 1$), linear ($R_L = 1$), favourable ($0 < R_L < 1$), or irreversible ($R_L = 0$). R_L values in this study were calculated to be in the range of 0.004–0.04. Hence, the adsorption of MG onto the CSAC adsorbent was found to be favourable.

Based on Table 2, the r^2 values for the Langmuir model were higher than for the Freundlich model at higher temperature. This observation indicates a tendency for the formation of MG monolayer on the CSAC surface at higher temperature. The occurrence of multilayer adsorption on the CSAC surface was highly possible at 303 K due to the good agreement with the Freundlich model. It is irrefutable that Q_m values have increased over increasing temperature. This could be associated with the increase in the availability of active sites for the adsorption at higher temperature [25]. The maximum monolayer adsorption capacity, Q_m of 78.11 mg/g was achieved at 323 K. The good fit between the experimental data to the Temkin model had produced a good correlation, where the r^2 values were greater than 0.9, which indicated the involvement of chemisorption in the MG/CSAC adsorption system. The heat of adsorption, B_T was found to increase more than 50 % with temperature increment.

3.8 Adsorption Kinetics

The non-linear Lagergren pseudo-first-order and pse-

Table 2. Two parameter adsorption isotherm models at 303, 313 and 323 K

Model	T (K)	Constants		r^2	SSE
Langmuir	303	K_L (L/mg)	0.46	0.970	2.391
$q_e = \frac{(Q_m K_L C_e)}{(1 + K_L C_e)}$		Q_m (mg/g)	61.83		
		R_L	0.04		
	313	K_L (L/mg)	1.64	0.997	0.781
		Q_m (mg/g)	70.78		
		R_L	0.01		
	323	K_L (L/mg)	4.57	0.999	0.438
		Q_m (mg/g)	78.11		
		R_L	0.004		
Freundlich	303	K_F (mg/g)(L/mg)$^{1/n}$	19.96	0.995	0.864
$q_e = K_F C_e^{(1/n)}$		n	2.04		
	313	K_F (mg/g)(L/mg)$^{1/n}$	42.82	0.965	2.492
		n	1.89		
	323	K_F (mg/g)(L/mg)$^{1/n}$	89.40	0.987	1.514
		n	1.74		
Temkin	303	b_t	242.89	0.987	0.864
$q_e = RT / b_T \ln (K_T C_e)$		K_T (L/g)	9.79		
		B_T (J/mol)	10.37		
	313	b_t	164.44	0.999	2.492
		K_T (L/g)	15.60		
		B_T (J/mol)	15.83		
	323	b_t	167.97	0.997	1.514
		K_T (L/g)	52.82		
		B_T (J/mol)	16.04		

udo-second-order kinetic equations are expressed by Eq. 9 and Eq. 10, respectively [30,31].

$$q_t = q_e(1 - e^{-K_1 t}) \quad (9)$$

$$q_t = \frac{q_e^2 K_2 t}{1 + q_e K_2 t} \quad (10)$$

where K_1 is expressed as the rate constant for the pseudo-first-order (1/min). K_2 is the rate constant of adsorption (g/(mg/min)). The fitting of the experimental data and the predicted model was evaluated based on non-linear error analysis.

Table 3 shows the kinetic model constants and the non-linear errors for the MG/CSAC adsorption system at 303 K, 313 K, and 323 K. The lower calculated r^2 and SSE values suggested that the MG/CSAC adsorption system was better fitted to the pseudo-second-order kinetic model. This indicates that the respective adsorption system was controlled by chemisorption. For all conditions, the calculated $q_{e,c}$ for the pseudo-second-order kinetic model were found to be higher than the $q_{e,cal}$ for the pseudo-first-order kinetic model. Additionally, the decreasing K_2 values over the increasing MG initial concentrations were reflected in the shorter time needed by the respective systems to achieve equilibrium at lower initial concentrations.

3.9 Intraparticle Diffusion

The intraparticle diffusion model is useful for identifying the diffusion mechanism based on the theory proposed by Weber and Morris [32]. The obtained adsorption kinetic data were analysed using Eq. 11:

$$q_t = k_{pi} t^{\frac{1}{2}} + C_i \quad (11)$$

where k_{pi} (mg/g min$^{1/2}$) is the intraparticle diffusion rate constant of stage i, which can be obtained from the plot of the straight line of q_t versus $t^{\frac{1}{2}}$. The intercept of stage i, C_i reflects the boundary layer effect on the respective system. If intraparticle diffusion occurs, the plot between q_t versus $t^{\frac{1}{2}}$ would form a linear line and passes through the origin. Otherwise, other mechanisms might also be involved in the adsorption process and the intraparticle diffusion is not the sole rate-limiting step. In general, intraparticle diffusion can be divided into three regions. The first, sharper region is the instantaneous adsorption process. The second region is the gradual adsorption, whereby the intraparticle diffusion is rate limiting. The third region is described as the final equilibrium stage that only happens in some cases. This region is where intraparticle diffusion starts to decrease because the number of adsorbates in the solutions would be extremely low [33].

Figure 11 shows the intraparticle diffusion plots for MG/CSAC adsorption system at 303 K, 313 K, and 323 K. As observed, the plots were non-linear over the whole time range. A similar trend was reported for the adsorp-

Table 3. Kinetic model constants and its non-linear errors for MG/CSAC adsorption system

T (K)	C_i	Pseudo 1st order kinetic				Pseudo 2nd order kinetic			
		K_1	$q_{e,c}$	r^2	SSE	K_2	$q_{e,c}$	r^2	SSE
303	10	0.2092	7.39	0.724	1.397	0.0278	7.98	0.819	1.129
	20	0.0910	15.41	0.823	2.595	0.0073	16.71	0.8933	1.889
	30	0.0372	24.59	0.902	3.197	0.0025	26.22	0.9359	2.351
	40	0.1111	27.41	0.767	5.295	0.0033	30.78	0.867	4.009
	50	0.1631	33.95	0.769	6.044	0.0044	37.18	0.8639	4.658
313	10	0.472	8.84	0.7975	1.166	0.0825	9.21	0.8827	0.844
	20	0.4497	17.55	0.7982	2.332	0.0390	18.29	0.881	1.705
	30	0.7249	25.03	0.7231	3.749	0.0411	26.18	0.8156	2.988
	40	0.4279	34.08	0.7731	4.934	0.0125	37.13	0.8671	3.949
	50	0.4898	42.77	0.7825	5.855	0.0176	44.54	0.8637	4.426
323	10	0.2064	8.71	0.7926	1.412	0.0281	9.33	0.8742	1.057
	20	0.2125	17.85	0.8345	2.501	0.0152	18.97	0.9069	1.788
	30	0.2225	25.44	0.7647	4.395	0.0099	27.34	0.8512	3.398
	40	0.1634	34.75	0.8025	5.757	0.0054	37.53	0.8797	4.303
	50	0.2234	42.11	0.7579	7.405	0.0032	49.09	0.8644	6.236

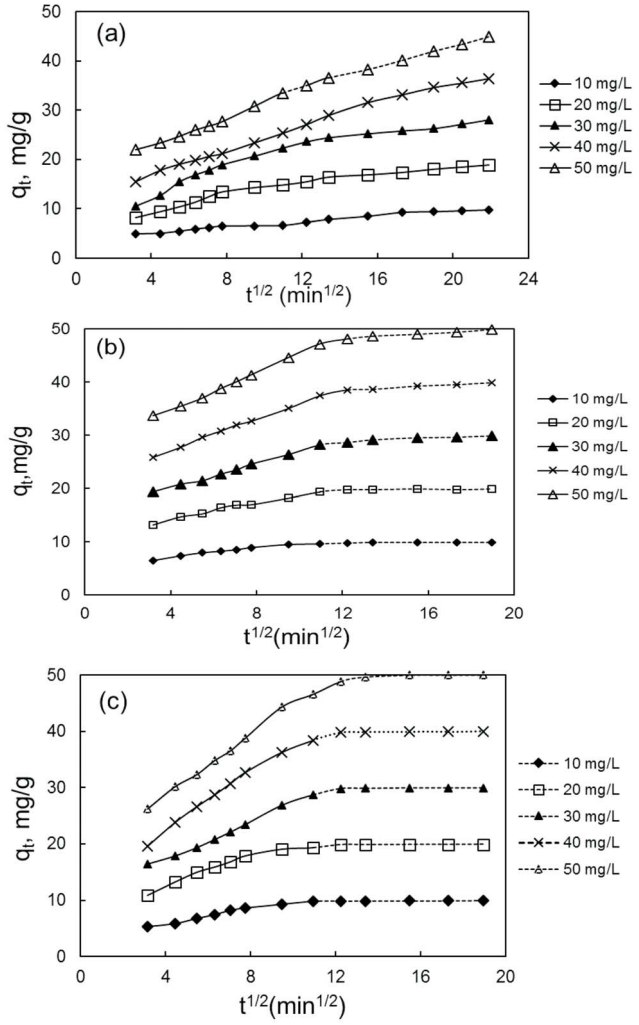

Figure 11. Intraparticle diffusion plots for MG/CSAC adsorption system at (a) 303 K, (b) 313 K, and (c) 323 K.

tion of MG on cellulose nanofibril aerogels [34]. At 323 K, the first stages of adsorption at lower initial concentrations (10 and 20 mg/L) and higher initial concentrations (30, 40, and 50 mg/L) were completed within the first 60 and 90 minutes, respectively. The second stage of intraparticle diffusion was attained before the third stage of equilibrium occurred. These different stages were influenced by the faster rate of adsorption during the initial process, which then slowed down as time increased. The linear lines of the first stage, second stage, and third stage did not pass through the origin, indicating that intraparticle diffusion was not the only rate-limiting step in the MG/CSAC adsorption system. The deviation from the origin could be due to the difference in the rate of mass transfer during the initial and final stages of dye adsorption [35]. Based on Table 4, the value of k_{pi} was found to increase when the concentration was increased from 10 mg/L to 50 mg/L. Increase in the adsorbate concentration had led to an increase in the MG diffusion rate due to the greater driving force. Furthermore, the values of C_i were also increased. This observation indicated that the boundary layer effect had increased with increasing MG initial concentration due to the large amount of solute being adsorbed at the boundary layer. A similar trend was described for the adsorption of methylene blue from aqueous solution onto pineapple leaf powder [36].

Further investigation was conducted using Boyd equation to determine the actual rate-controlling step in the MG/CSAC adsorption system. The equation for Boyd

Table 4. Intraparticle diffusion model constant and correlation coefficients for MG/CSAC adsorption system at 303 K, 313 K, and 323 K

Temperature (K)	Initial concentration (mg/L)	k_{p1} (mg/g $min^{1/2}$)	C_1	R_1	k_{p2} (mg/g $min^{1/2}$)	C_2	R_2	k_{p3} (mg/g $min^{1/2}$)	C_3	R_3
303	10	0.375	3.514	0.955	0.275	4.07	0.957	-	-	-
	20	1.142	4.349	0.989	0.385	10.751	0.983	-	-	-
	30	1.419	7.128	0.968	0.425	18.567	0.984	-	-	-
	40	1.252	11.855	0.995	0.865	17.913	0.982	-	-	-
	50	1.486	16.727	0.995	0.990	23.12	0.997	-	-	-
313	10	0.514	5.030	0.984	0.183	7.652	0.909	0.0123	9.689	0.747
	20	0.861	10.716	0.965	0.627	12.261	0.978	0.022	19.512	0.7051
	30	1.123	15.715	0.993	0.670	20.4	0.904	0.133	27.42	0.941
	40	1.463	2.423	0.996	0.927	26.777	0.8786	0.224	35.718	0.994
	50	1.775	27.654	0.998	0.583	40.871	0.983	0.224	45.586	0.991
323	10	0.767	2.644	0.988	0.389	5.585	0.999	0.012	9.714	0.8364
	20	1.492	6.416	0.994	0.406	14.946	0.939	0.011	19.716	0.930
	30	1.672	10.555	0.987	1.057	16.957	0.992	0.017	29.63	0.801
	40	2.654	11.778	0.994	1.265	24.371	0.992	0.025	39.504	0.7746
	50	2.813	17.154	0.996	1.394	31.282	0.977	0.058	48.933	0.692

model is presented by Eq. 12:

$$B_t = -0.4977 - \ln(1 - F) \quad (12)$$

where F is the fraction of solute absorbed at any time, t (h) and it is calculated using Eq. 13:

$$F = \frac{q_t}{q_o} \quad (13)$$

The plot of B_t versus time is a linear line passing through the origin when the adsorption rate is governed by the particle diffusion mechanism. Otherwise, it is governed by the film diffusion mechanism [37]. The plots of Boyd model for the adsorption of MG on CSAC at 303 K, 313 K, and 323 K are shown by Figure 12. A thorough inspection revealed that the plotted linear lines, for all initial MG concentrations, did not pass through the origin. This indicated that the adsorption of MG on CSAC was mainly governed by film diffusion mechanism.

3.10 Thermodynamics

The thermodynamic parameters, such as Gibbs energy (ΔG°), change in enthalpy (ΔH°), and change in entropy (ΔS°) were evaluated using the following Eq. 14 and Eq. 15 [38]:

$$\Delta G° = RT \ln K \quad (14)$$
$$\ln K = (\Delta S°) / R - (\Delta H°) / RT \quad (15)$$

where K is the distribution coefficient (L/mg), R is the universal gas constant at 8.314 J (mol K)$^{-1}$, and T is the temperature in K. The values of $\Delta H°$ and $\Delta S°$ were determined from the slope and intercept of Van't Hoff plot of ln K versus $1/T$ (graph not shown).

Negative values of $\Delta G°$ obtained at 313 K ($\Delta G°$ = -1.28 kJ/mol) and 323 K ($\Delta G°$ = -4.08 kJ/mol) indicated that the MG/CSAC adsorption system was spontaneous in nature at higher temperature. This could be explained by the fact that the mobility of the adsorbates in the solution and their affinity for the adsorbent had increased with increasing temperature [39]. The positive values of $\Delta H°$ (93.84 kJ/mol) and $\Delta S°$ (303.41 J/mol/K) indicated the endothermic nature of MG adsorption, and reflected the affinity of the MG adsorbates towards CSAC. To further interpret the nature of MG adsorption on CSAC, the Arrhenius expression was applied to determine the minimum energy required by the reactant for the reaction to proceed. The Arrhenius expression is defined by the following Eq. 16:

$$\ln K_2 = -\frac{E_a}{RT} + \ln A \quad (16)$$

where K_2 and E_a (kJ/mol) are the pseudo-second-order rate constant and activation energy, respectively. The value of the Arrhenius activation energy can be obtained

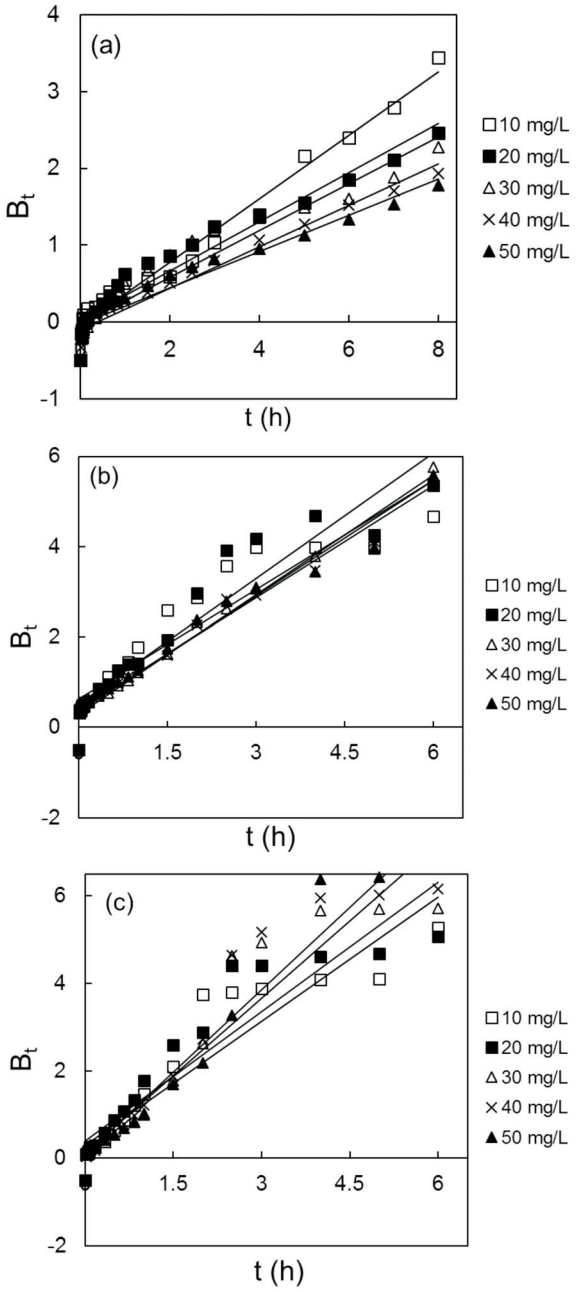

Figure 12. Boyd plots for adsorption of MG/CSAC adsorption system (a) 303 K, (b) 313 K, and (c) 323 K.

from the slope of the linear plot of ln K_2 versus $1/T$. If E_a value is < 40 kJ/mol, the process would have involved physisorption, while E_a value > 40 kJ/mol would indicate that the adsorption process had occurred via chemisorption [40]. Hence, chemisorption was suggested to dominantly govern the MG/CSAC adsorption system, based on the calculated E_a of 93.49 kJ/mol.

4. Conclusions

The adsorption and desorption of MG using CSAC has been studied in this work. The CSAC has demonstrated favourable characteristics for removing MG from an aqueous phase. The MG adsorption data on CSAC was well represented by Langmuir, Freundlich, and Temkin adsorption isotherm models. A good fit to the pseudo-second-order kinetic model was obtained for the chemisorption occurrence in the MG/CSAC adsorption system. Intraparticle diffusion was not the sole rate-limiting step in the adsorption of MG on CSAC. Film diffusion was proposed as playing a significant role in governing the MG/CSAC adsorption system. The thermodynamic properties revealed that the adsorption was spontaneous and endothermic in nature. In conclusion, CSAC has demonstrated good reusability properties, with the ability to sustain the removal efficiency of MG > 89% upon the completion of five consecutive adsorption/desorption cycles.

Acknowledgements

This current work was financially supported by a short-term research grant (Project Number: 304/PJKIMIA/60313025), provided by Universiti Sains Malaysia.

References

[1] Robinson, T., McMullan, G., Marchant, R. and Nigam, P., "Remediation of Dyes in Textile Effluent: a Critical Review on Current Treatment Technologies with a Proposed Alternative," *Bioresource Technology*, Vol. 77, No. 3, pp. 247–255 (2001). doi: 10.1016/S0960-8524(00)00080-8

[2] Chowdhury, S., Mishra, R., Saha, P. and Kushwaha, P., "Adsorption Thermodynamics, Kinetics and Isosteric Heat of Adsorption of Malachite Green onto Chemically Modified Rice Husk," *Desalination*, Vol. 265, No. 1, pp. 159–168 (2011). doi: 10.1016/j.desal.2010.07.047

[3] Tran, H. N., Wang, Y. F., You, S. J. and Chao, H. P., "Insights into the Mechanism of Cationic Dye Adsorption on Activated Charcoal: the importance of π–π Interactions," *Process Safety and Environmental Protection*, Vol. 107, pp. 168–180 (2017). doi: 10.1016/j.psep.2017.02.010

[4] Méndez, A., Fernández, F. and Gascó, G., "Removal of Malachite Green Using Carbon-based Adsorbents," *Desalination*, Vol. 206, No. 1–3, pp. 147–153 (2007). doi: 10.1016/j.desal.2006.03.564

[5] Makeswari, M. and Santhi, T., "Removal of Malachite Green Dye from Aqueous Solutions onto Microwave Assisted Zinc Chloride Chemical Activated Epicarp of Ricinus Communis," *Journal of Water Resource and Protection*, Vol. 5, No. 2, p. 222 (2013). doi: 10.4236/jwarp.2013.52023

[6] Saha, P., Chowdhury, S., Gupta, S., Kumar, I. and Kumar, R., "Assessment on the Removal of Malachite Green Using Tamarind Fruit Shell as Biosorbent," *Clean: Soil, Air, Water*, Vol. 38, No. 5–6, pp. 437–445 (2010). doi: 10.1002/clen.200900234

[7] Srivastava, S., Sinha, R. and Roy, D., "Toxicological Effects of Malachite Green," *Aquatic Toxicology*, Vol. 66, No. 3, pp. 319–329 (2004). doi: 10.1016/j.aquatox.2003.09.008

[8] Abou-Gamra, Z. M. and Ahmed, M. A., "TiO2 Nanoparticles for Removal of Malachite Green Dye from Waste Water," *Advances in Chemical Engineering and Science*, Vol. 3, p. 373 (2015). doi: 10.4236/aces.2015.53039

[9] Han, R., Zhang, J., Zou, W., Shi, J. and Liu, H., "Equilibrium Biosorption Isotherm for Lead Ion on Chaff," *Journal of Hazardous Materials*, Vol. 125, No. 1, pp. 266–271 (2005). doi: 10.1016/j.jhazmat.2005.05.031

[10] Gupta, V. K., Ali, I. and Mohan, D., "Equilibrium Uptake and Sorption Dynamics for the Removal of a Basic Dye (Basic Red) Using Low-cost Adsorbents," *Journal of Colloid and Interface Science*, Vol. 265, No. 2, pp. 257–264 (2003). doi: 10.1016/S0021-9797(03)00467-3

[11] Sari, A., Mendil, D., Tuzen, M. and Soylak, M., "Bio-

sorption of Cd (II) and Cr (III) from Aqueous Solution by Moss (Hylocomium Splendens) Biomass: Equilibrium, Kinetic and Thermodynamic Studies," *Chemical Engineering Journal*, Vol. 144, No. 1, pp. 1–9 (2008). doi: 10.1016/j.cej.2007.12.020

[12] Kumar, K. V., "Comparative Analysis of Linear and Non-linear Method of Estimating the Sorption Isotherm Parameters for Malachite Green onto Activated Carbon," *Journal of Hazardous Materials*, Vol. 136, No. 2, pp. 197–202 (2006). doi: 10.1016/j.jhazmat.2005.09.018

[13] Ho, Y. S., "Second-order Kinetic Model for the Sorption of Cadmium onto Tree Fern: a Comparison of Linear and Non-linear Methods," *Water Research*, Vol. 40, No. 1, pp. 119–125 (2006). doi: 10.1016/j.watres.2005.10.040

[14] Foo, K. Y. and Hameed, B. H., "Insights into the Modeling of Adsorption Isotherm Systems," *Chemical Engineering Journal*, Vol. 156, No. 1, pp. 2–10 (2010). doi: 10.1016/j.cej.2009.09.013

[15] Gupta, V. K., "Application of Low-cost Adsorbents for Dye Removal–a Review," *Journal of Environmental Management*, Vol. 90, No. 8, pp. 2313–2342 (2009). doi: 10.1016/j.jenvman.2008.11.017

[16] Djebri, N., Boutahala, M., Chelali, N. E., Boukhalfa, N. and Zeroual, L., "Enhanced Removal of Cationic Dye by Calcium Alginate/organobentonite Beads: Modeling, Kinetics, Equilibriums, Thermodynamic and Reusability Studies," *International Journal of Biological Macromolecules*, Vol. 92, pp. 1277–1287 (2016). doi: 10.1016/j.ijbiomac.2016.08.013

[17] Hidayu, A. R., Mohamad, N. F., Matali, S. and Sharifah, A. S., "Characterization of Activated Carbon Prepared from Oil Palm Empty Fruit Bunch Using BET and FT-IR Techniques," *Procedia Engineering*, Vol. 68, pp. 379–384 (2013). doi: 10.1016/j.proeng.2013.12.195

[18] Vilella, P. C., Lira, J. A., Azevedo, D. C. S., Bastos-Neto, M. and Stefanutti, R., "Preparation of Biomass-based Activated Carbons and Their Evaluation for Biogas Upgrading Purposes," *Industrial Crops & Products*, Vol. 109, pp. 134–140 (2017). doi: 10.1016/j.indcrop.2017.08.017

[19] Tan, Y. L., Islam, M. A., Asif, M. and Hameed, B. H., "Adsorption of Carbon Dioxide by Sodium Hydroxide-modified Granular Coconut Shell Activated Carbon in a Fixed Bed," *Energy*, Vol. 77, pp. 926–931 (2014). doi: 10.1016/j.energy.2014.09.079

[20] Shayesteh, H., Rahbar-Kelishami, A. and Norouzbeigi, R., "Adsorption of Malachite Green and Crystal Violet Cationic Dyes from Aqueous Solution Using Pumice Stone as a Low-cost Adsorbent: Kinetic, Equilibrium, and Thermodynamic Studies," *Desalination and Water Treatment*, Vol. 57, No. 27, pp. 12822–12831 (2016). doi: 10.1080/19443994.2015.1054315

[21] Ahmad, R. and Kumar, R., "Adsorption Studies of Hazardous Malachite Green onto Treated Ginger Waste," *Journal of Environmental Management*, Vol. 91, No. 4, pp. 1032–1038 (2010). doi: 10.1016/j.jenvman.2009.12.016

[22] Agarwal, S., Tyagi, I., Gupta, V. K., Mashhadi, S. and Ghasemi, M., "Kinetics and Thermodynamics of Malachite Green Dye Removal from Aqueous Phase Using Iron Nanoparticles Loaded on Ash" *Journal of Molecular Liquids*, Vol. 223, pp. 1340–1347 (2016). doi: 10.1016/j.molliq.2016.04.039

[23] Barka, N., Qourzal, S., Assabbane, A., Nounah, A. and Yhya, A. I., "Adsorption of Disperse Blue SBL Dye by Synthesized Poorly Crystalline Hydroxyapatite," *Journal of Environmental Sciences*, Vol. 20, No. 10, pp. 1268–1272 (2008). doi: 10.1016/S1001-0742(08)62220-2

[24] Crini, G., Peindy, H. N., Gimbert, F. and Robert, C., "Removal of CI Basic Green 4 (Malachite Green) from Aqueous Solutions by Adsorption Using Cyclodextrin-based Adsorbent: Kinetic and Equilibrium Studies," *Separation and Purification Technology*, Vol. 53, No. 1, pp. 97–110 (2007). doi: 10.1016/j.seppur.2006.06.018

[25] Sepehr, M. N., Amrane, A., Karimaian, K. A., Zarrabi, M. and Ghaffari, H. R., "Potential of Waste Pumice and Surface Modified Pumice for Hexavalent Chromium Removal: Characterization, Equilibrium, Thermodynamic and Kinetic Study," *Journal of the Taiwan Institute of Chemical Engineers*, Vol. 45, No. 2, pp. 635–647 (2014). doi: 10.1016/j.jtice.2013.07.005

[26] Guz, L., Curutchet, G., Sánchez, R. T. and Candal, R., "Adsorption of Crystal Violet on Montmorillonite (or Iron Modified Montmorillonite) Followed by Degradation through Fenton or Photo-Fenton Type Reactions," *Journal of Environmental Chemical Engineer-*

ing, Vol. 2, No. 4, pp. 2344–2351 (2014). doi: 10.1016/j.jece.2014.02.007

[27] Neupane, S., Ramesh, S. T., Gandhimathi, R. and Nidheesh, P. V., "Pineapple Leaf (Ananas Comosus) Powder as a Biosorbent for the Removal of Crystal Violet from Aqueous Solution," *Desalination Water Treatment*, Vol. 54, No. 7, pp. 2041–2054 (2015). doi: 10.1080/19443994.2014.903867

[28] Liu, Q., Wang, L., Xiao, A., Yu, H. and Ericson, M., "Regeneration Research of Porous Magnetic Microspheres during Treatment of Wastewater Containing Cationic Dyes," *Separation Science and Technology*, Vol. 45, No. 16, pp. 2345–2349 (2010). doi: 10.1080/01496395.2010.504453

[29] Mohd-Din, A. T., Ahmad, M. A. and Hameed, B. H., "Ordered Mesoporous Carbons Originated from Nonedible Polyethylene Glycol 400 (PEG-400) for Chloramphenicol Antibiotic Recovery from Liquid Phase," *Chemical Engineering Journal*, Vol. 260, pp. 730–739 (2015). doi: 10.1016/j.cej.2014.09.010

[30] Ho, Y. S. and McKay, G., "Sorption of Dye from Aqueous Solution by Peat," *Chemical Engineering Journal*, Vol. 70, No. 2, pp. 115–124 (1998). doi: 10.1016/S0923-0467(98)00076-1

[31] Ho, Y. S., "Review of Second-order Models for Adsorption Systems," *Journal of Hazardous Materials*, Vol. 136, No. 3, pp. 681–689 (2006). doi: 10.1016/j.jhazmat.2005.12.043

[32] Weber, W. J. and Morris, J. C., "Kinetics of Adsorption on Carbon from Solution," *Journal of the Sanitary Engineering Division*, Vol. 89, No. 2, pp. 31–60 (1963). http://cedb.asce.org/CEDBsearch/record.jsp?dockey=0013042

[33] Cheung, W. H., Szeto, Y. S. and McKay, G., "Intraparticle Diffusion Processes during Acid Dye Adsorption onto Chitosan," *Bioresource Technology*, Vol. 98, No. 15, pp. 2897–2904 (2007). doi: 10.1016/j.biortech.2006.09.045

[34] Jiang, F., Dinh, D. M. and Hsieh, Y. L., "Adsorption and Desorption of Cationic Malachite Green Dye on Cellulose Nanofibril Aerogels," *Carbohydrate Polymers*, Vol. 173, pp. 286–294 (2017). doi: 10.1016/j.carbpol.2017.05.097

[35] Tan, I. A., Ahmad, A. L. and Hameed, B. H., "Adsorption Isotherms, Kinetics, Thermodynamics and Desorption Studies of 2,4,6-trichlorophenol on Oil Palm Empty Fruit Bunch-based Activated Carbon," *Journal of Hazardous Materials*, Vol. 164, No. 2, pp. 473–482 (2009). doi: 10.1016/j.jhazmat.2008.08.025

[36] Weng, C. H., Lin, Y. T. and Tzeng, T. W., "Removal of Methylene Blue from Aqueous Solution by Adsorption onto Pineapple Leaf Powder," *Journal of Hazardous Materials*, Vol. 170, No. 1, pp. 417–424 (2009). doi: 10.1016/j.jhazmat.2009.04.080

[37] Tang, B., Lin, Y., Yu, P. and Luo, Y., "Study of Aniline/ε-caprolactam Mixture Adsorption from Aqueous Solution onto Granular Activated Carbon: Kinetics and Equilibrium," *Chemical Engineering Journal*, Vol. 187, pp. 69–78 (2012). doi: 10.1016/j.cej.2012.01.088

[38] Bouaziz, F., Koubaa, M., Kallel, F., Ghorbel, R. E. and Chaabouni, S. E., "Adsorptive Removal of Malachite Green from Aqueous Solutions by Almond Gum: Kinetic Study and Equilibrium Isotherms," *International Journal of Biological Macromolecules*, Vol. 105, pp. 56–65 (2017). doi: 10.1016/j.ijbiomac.2017.06.106

[39] Saha, P. and Chowdhury, S., "Insight into Adsorption Thermodynamics," *Thermodynamics*, Prof. Mizutani Tadashi (Ed.), InTech, pp. 349–364 (2011). doi: 10.5772/13474

[40] Banerjee, S., Sharma, G. C., Gautam, R. K., Chattopadhyaya, M. C., Upadhyay, S. N. and Sharma, Y. C., "Removal of Malachite Green, a Hazardous Dye from Aqueous Solutions Using Avena Sativa (oat) Hull as a Potential Adsorbent," *Journal of Molecular Liquids*, Vol. 213, pp. 162–172 (2016). doi: 10.1016/j.molliq.2015.11.011

Manuscript Received: Nov. 16, 2017
Accepted: Apr. 16, 2018